Computational Intelligence in Electrical Engineering
Vol. 14, No. 4, 2024
pp. 1-16
Research Paper

Online state estimation of power system despite faulty measurement data using the composition of ANFIS with Grasshopper Algorithm

Arash Esmaili[1], Asghar Akbari Foroud [2]*

[1] Power department, electrical and computer engineering faculty, Semnan University, Semnan, Iran
aesmaili@semnan.ac.ir
[2] Power department, electrical and computer engineering faculty, Semnan University, Semnan, Iran
aakbari@semnan.ac.ir

Abstract :
In this paper, we propose a novel state estimation plan using Adaptive Neuro-Fuzzy Inference System (ANFIS). To increase the speed and accuracy of estimation, an individual ANFIS is used for each bus. To improve the accuracy of training, the grasshopper optimization algorithm (GOA) is used for the training and optimization of ANFIS parameters. The main advantage of GOA training of ANFIS parameters is the increase in speed and accuracy in estimating power system state variables. One of the main features of the proposed design is its ability to provide an appropriate state estimation when incomplete data is sent to the control center due to the disconnection of communication or the failure of the measurement devices. The recovery of the missed data is implemented by the Group Method of Data Handling (GMDH) neural network. The GMDH neural network is widely used due to its proper speed for function estimation and approximation. Incomplete information obtained from measurements to estimate the state is processed by the GMDH neural network to recover lost information. The output of this neural network, which is the retrieval of complete measurement information, is given to ANFIS to estimate the state of the power system as input.

Keywords: State estimation, Adaptive Neuro-Fuzzy Inference System (ANFIS), Grasshopper optimization algorithm, Group Method of Data Handling (GMDH) eural network.

1. Introduction

State estimation is the process of determining the state of the system. Identifying the present operating state of a system needs to state estimation [1].

Today, most power systems use data in state estimation that are collected and sent to the network's control and operation centers by Supervisory Control and Data Acquisition (SCADA) system. The measurements include the power flow of the lines, power injection at the buses, and voltage and current magnitudes. As data refreshes from the

[1] Submission date:08, 11, 2022
Acceptance date: 10, 04, 2023
Corresponding author: Asghar Akbari Foroud, Power department, electrical and computer engineering faculty, Semnan university

https://doi.org/10.22108/ISEE.2023.135667.1596

SCADA systems are typically done every 2–4s, instantaneous visibility of the system is not possible. In more modern systems, the phasor measurement units (PMUs) can be used to collect and send data, which leads to improving the speed and accuracy of state estimation. With PMUs, data can be measured more than 30 times per second, rather than once every few seconds. However, the use of PMU measurement units is principally linked with high costs and narrow bandwidth of communication channel [2, 3]. Since PMUs are rather expensive devices, a limited number of PMUs is required to make the system entirely observable [4-9].

The Weighted Least Squares (WLS) algorithm is one of the basic and fundamental algorithms for state estimation. The accuracy of the WLS estimator relies on the measurements available for state estimation [10]. When the system suffers some measurement interruptions, due to device or transmission failure, the use of the WLS estimator does not lead to satisfactory results [11]. On the other hand, The WLS is a nonlinear and recursion calculation method, which increases the time of state estimation [12]. This time in large systems may take more than a few minutes, so the system is not instantly observable and the visibility of the power system is updated every few minutes.

The objective function of the state estimator is nonlinear and asymmetric with regard to the presence of nonlinear power devices such as large compensators, generators, and transformers with different taps, thereby making the classical approaches inefficient to obtain the optimal values of the nonlinear objective function. To overcome the limitations of classical optimization methods, artificial intelligence techniques, evolutionary algorithms, neural networks, and fuzzy networks have been considered new tools for estimating power system states [13, 14, 15].

The hybrid method presented in [16] for power system state estimation, consists of a Cellular Computational Network (CCN) and the Genetic Algorithm (GA). CCN is a computational algorithm, that is implemented for state estimation in that paper and its result is further improved using GA. Up to now, optimization algorithms have been used in various topics, including state estimation and load prediction [17, 18]. Particle Swarm Optimization (PSO) is a powerful meta-optimization algorithm that was used in three-phase state estimation [19]. PSO is a repetition-based algorithm and when using this algorithm in large-scale power systems, the time of estimation takes about ten minutes, which is a long time. However, the use of this method is possible when the network is not very large or high-speed state estimation is not necessary. In [20], the state estimation is presented using the combination of WLS methods and the weighted least absolute value (WLAV) with some optimization algorithms such as Genetic Algorithm (GA) and Bee Colony algorithm, and PSO, ..., and the results are compared to each other. Optimization algorithms implemented in that paper, minimize the measurement errors.

The use of neural networks such as Hopfield neural network (HNN) for state estimation was studied in [21]. The main advantage of artificial neural network-based estimators, despite errors in measurements, is that they can achieve more appropriate results at a faster rate than the WLS estimators [14]. The Radial Basis Function (RBF) network is a type of artificial neural network that has been introduced in some papers for application to problems of state estimation [22, 23]. The Multi-Layer Perceptron Neural Network (MLP) is one of the most widely used neural networks in different fields such as approximation, prediction, and estimation of functions. These networks are suitable for small power systems [24, 25]. Deep learning networks such as AutoEncoders and Convolutional Networks are some kind of neural networks that have attracted more attention since the year 2012. These types of neural networks are most commonly used in the image, text, and audio processing. However, these types of neural networks are also used for power system state estimation [26-29]. In [30], the neural network employs the measured mixed data of PMU and SCADA units as input to estimate the state with higher accuracy. Principal component analysis (PCA) is a well-known statistical procedure for reducing data dimensions. This method is a part of the preprocess for neural networks which has the advantages such as the elimination of redundant data; hence the speed of the process can be increased. PCA is adopted for processing the hybrid data collected by SCADA and PMUs and eliminates outliers [30, 31].

Determination of optimal parameter values of the neural networks like that MLP and RBF by using the optimization algorithms such as GA and PSO is counted as one of the optimization problems in applications such as load forecasting and state estimation. Through combination of neural networks with optimization algorithms, the network will be better trained and thus the prediction error or estimation error will decrease [32-36]. Determining the values of the MLP neural network parameters with the Stochastic Fractal Search (SFS) algorithm and Differential Evolution (DE) has led to a more accurate state estimation [15, 37].

Another all-purpose dynamic state estimator, Kalman filter, is easily implemented and able to predict the state of the system. Kalman filter is a recursive filter and needs to the output of its previous state estimation and present data to estimate the current state variables. The equation for the Kalman filter is divided into two steps: predict and update. In the prediction step, estimates of the current state variables are produced via using the past estimations. In the update step, data and measurements of the current state are integrated with the previous estimate results [38], [39], [40].

In this paper, a new plan is proposed for state estimation of the power system in normal condition, as well as when there is insufficient data, due to the problem in the meter or the disconnection. ANFIS is the main estimation tool in this plan. To increase the estimation speed and accuracy, we use a individual ANFIS for each bus which actually represents parallel processing. ANFIS mainly can be trained by means of classic techniques. In this plan, a meta-optimization algorithm namely grasshopper optimization algorithm, is used to train and optimize the ANFIS parameters. Another feature of the proposed plan is that, in addition to normal condition, it can provide an appropriate estimation when the incomplete data sent to the control center due to the disconnection of communication or the failure of the measurement devices. As the state estimation is performed in a short time, the missed data recovery must be carried out as soon as possible; therefore, the recovery of missed measurements is done by the Group Method of Data Handling (GMDH). The GMDH neural network is widely used for functions estimation and approximation due to the appropriate speed. With regards to its high performance speed, the proposed plan can also be used in online state estimation.

The contributions of this paper are summarized as follows:

1) Using measurement division method to improve the accuracy and speed of state estimation done by ANFIS.

2) Using the Grasshopper Optimization Algorithm (GOA) to obtain the optimal parameters settings of ANFIS with the aim of increasing the accuracy of power system state estimation.

3) Effectiveness of the proposed plan with incomplete data. Recovery of these data by means of the GMDH neural network is done in the shortest time.

4) Suitability of the proposed plan for large power systems, as well as online mode estimation due to its high speed and accuracy.

The remainder of this paper is structured as follows. Section 2, describes the ANFIS. Section 3, presents the descriptions and relations of the GOA optimization algorithm. Section 4, investigates the proposed method. Section 5 is allocated to examine the results of the proposed plan in incomplete data conditions. Section 6 compares the proposed plan with several other methods and section 7 outlines the work process and conclusions. The proposed state

estimation plan has been tested on the IEEE 14-bus and 118-bus modified test systems.

2-Adaptive Neuro-Fuzzy Inference System (ANFIS)

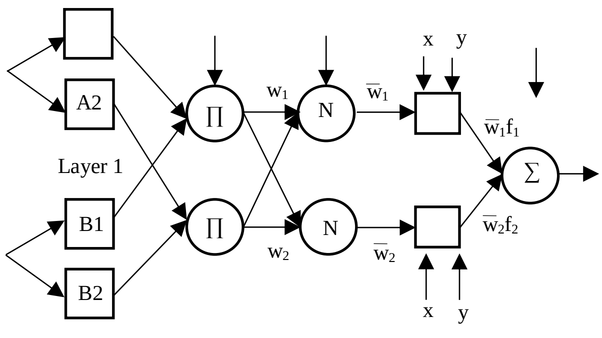

Fig. 1. Fuzzy Neural Network

An adaptive neuro-fuzzy inference system or adaptive network-based fuzzy inference system (ANFIS) is a kind of artificial neural network and based on Takagi–Sugeno fuzzy inference system [41,42]. An ANFIS is a kind of artificial neural network that based on first- order Takagi–Sugeno fuzzy inference system. First- order means that the rules established in the system are a linear combination of the inputs. ANFIS network is a set of "if-then" rules that have learning capability to approximate nonlinear functions [43,44]. Hence, the ANFIS has been considered as an estimator [45]. A simple two inputs and a single output of ANFIS structure is shown in Fig1.

In the first layer, the output of node is defined by (1):

$$O_i^1 = \mu_{A_i}(x) \tag{1}$$

where, x is input to node and A_i is the fuzzy set. $\mu_{A_i}(x)$ is the membership of x and it determines the degree to which the input belongs to the fuzzy set A_i.

Membership functions are selected according to the type of problem and function (2) is one of the widely used membership functions.

$$\mu_{A_i}(\boldsymbol{x}) = \frac{\mathbf{1}}{\mathbf{1} + \left|\frac{\boldsymbol{x} - \boldsymbol{r_i}}{\boldsymbol{p_i}}\right|^{2q_i}} \tag{2}$$

r_i, p_i and q_i are the parameters of membership function. The parameters of the membership functions are specified in the ANFIS training process. The first layer is called the fuzzy layer. In the second layer, multiplication is performed between all inputs. The nodes of this layer determine the fire rate of each rule. The output of this layer is characterized by w_i .

$$O_i^2 = w_i = \prod_j \mu_j = \mu_{A_i}(x).\mu_{B_i}(y) \quad i = 1,2 \tag{3}$$

In the third layer, the fire rate of each rule is normalized as:

$$O_i^3 = \overline{w}_i = \frac{w_i}{\sum_j w_j} \quad i,j = 1,2 \tag{4}$$

In the fourth layer, weighted outputs for normalized rules are calculated as:

$$O_i^4 = \overline{w}_i f_i = \overline{w}_i(a_i x + b_i x + c_i) \tag{5}$$

The values a_i, b_i and c_i are set in the ANFIS tutorial process. This layer acts like a neuron in the neural network. In the fifth layer, the linear summation of the outputs of the fourth layer is calculated as the output [47]:

$$O_i^5 = \sum \overline{w}_i f_i \tag{6}$$

Normally one of two indexes namely mean squared error or mean absolute percentage error is used to check the error rate of the fuzzy neural network, whether in the training section or in the operation section. The larger indicators represent the larger error in the process of state estimation.
The mean squared error and mean absolute percentage error are defined in equations (7) and (8) respectively:

$$\text{MSE} = \frac{\sum_{t=1}^{n}(\boldsymbol{e_t})^2}{\boldsymbol{n}} = \frac{\sum_{t=1}^{n}\left(\boldsymbol{A_t} - \overline{\boldsymbol{A}}_t\right)^2}{\boldsymbol{n}} \tag{7}$$

$$\text{MAPE} = \frac{\sum_{t=1}^{n}\left|\frac{e_t}{A_t}\right|}{n} \times 100 = \frac{\sum_{t=1}^{n}\left|\frac{A_t - \bar{A}_t}{A_t}\right|}{n} \times 100 \tag{8}$$

A_t is the measured actual value of the variable, and $\bar{A}_t$ is the estimated value.

3. Optimization Algorithms

Basically, an optimization problem is solved in the ANFIS training process. The purpose of ANFIS training is to determine the optimal values of ANFIS parameters in each layer. The conventional method for setting ANFIS parameters is the Gradient descent method. In this paper, the Gradient descent method is being replaced by the grasshopper optimization algorithm. The main advantage of the grasshopper optimization algorithm is to obtain better general points than Gradient descent-based algorithms. The Grasshopper optimization algorithm is one of the newest evolutionary and meta-algorithms that is introduced as a new optimization algorithm that mimics the behavior of the grasshopper during the migration and searches for food. To simulate the behavior of grasshoppers, we use the following mathematical model:

$$X_i = S_i + G_i + A_i \tag{9}$$

where X_i is the position, S_i is the social interaction, G_i is the gravity force on the i-th grasshopper and A_i shows the wind advection. To provide random behavior, we can write equation (9) as:

$$X_i = r_1 S_i + r_2 G_i + r_3 A_i \tag{10}$$

where r_1, r_2 and r_3 are random numbers in the interval [0, 1]. The value of S_i is calculated as follows:

$$S_i = \sum_{\substack{j=1 \\ j \neq i}}^{N} S(d_{ij})\widehat{d_{ij}} \quad (11)$$

d_{ij} is the distance between the i-th and j-th grasshopper and is determined as $d_{ij} = |x_i - x_j|$ and $\hat{d}_{ij} = \left|\frac{x_i - x_j}{d_{ij}}\right|$. *N* is the number of grasshoppers. *S* is a function for defining the social forces and formulated as equation (12):

$$S(r) = f e^{\frac{-r}{l}} - e^{-r} \quad (12)$$

where *f* and *I* show the intensity of attraction and the attractive length scale respectively. We consider *f* = 0.5 and *I* = 1.5. Comfortable distance in the grasshopper optimization algorithm is the distance between two grasshoppers without attraction and repulsion. G_i component is calculated as:

$$G_i = -g\hat{e}_g \quad (13)$$

where g is the gravitational constant and $\hat{e}_g$ is a unity vector towards the center of the earth. Using equation (14), the component A is determined:

$$A_i = u\hat{e}_w \quad (14)$$

where *u* is a constant drift and $\hat{e}_g$ indicates a unity vector in the direction of the wind. The direction of the wind is always towards the objective function. Substituting *S*, *G*, *A* from equations 11, 13 and 14 in equation 9, we can obtain equation 15:

$$X_i = \sum_{\substack{j=1 \\ j \neq i}}^{N} S(|x_j - x_i|)\frac{x_j - x_i}{d_{ij}} - g\hat{e}_g + u\hat{e}_w \quad (15)$$

This mathematical model cannot be used directly to solve optimization problems. A modified version of

this equation is proposed as follows to solve optimization problems:

$$X_i^d = c\left(\sum_{\substack{j=1 \\ j \neq i}}^{N} c\frac{ub_d - lb_d}{2} S(|x_j^d - x_i^d|)\frac{x_j - x_i}{d_{ij}}\right) + \hat{T}_d \quad (16)$$

where ub_d and lb_d are the upper and lower bounds in d-th dimension respectively. $\hat{T}_d$ shows the best-founded solution and *c* is the decreasing factor to reduce the repulsion zone, comfort zone and attraction zone. For balancing exploration and exploitation, parameter c should be reduced proportional to the number of iteration and it is calculated as follows:

$$c = cmax - l\frac{cmax - cmin}{L} \quad (17)$$

where cmax and cmin are the maximum and minimum values of c respectively. l indicate the current iteration and L is the total number of iterations. cmax =1 and cmin =0.00001 [48].

4. The proposed plan for state estimation

In this paper, we propose a new plan for power systems state estimation. Voltage magnitudes and angles at each bus are the power system state variables. Details of the proposed plan are as follows: In this plan, an ANFIS is used to estimate the state. To increase the speed and accuracy of the state estimation process, the measurement division method is used. In a large-scale power system, the number of state variables and therefore, the number of measured variables for state variable estimation are too high. Estimating a large number of state variables by an ANFIS causes to increase in the size of the ANFIS. The increase in the size of ANFIS is accompanied by an increase in network parameters and this in turn, reduces the convergence rate in the training process and reduces accuracy for both training and state estimation. One of the proposed methods for a system with large measured data is the measurement division technique (Figure 2).

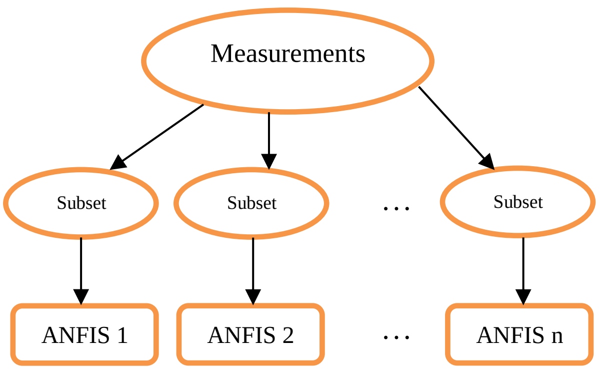

Figure. 2. Measurement division technique

The measurement division technique refers to the concept that the total measurements are divided into several subsets, so that measurement data processing can be done with more speed and accuracy.

In this proposed plan, measurements for each bus are placed in an individual set and an ANFIS is used to estimate the state variables of each bus. The needed measurements for power systems state estimation include active and reactive power injected into the bus and the active and reactive power flow of the lines connected to each bus (Figure 2). In this method, a significant decrease in the number of ANFIS parameters results in more training speed. Certainly, increasing accuracy also occurs with decreasing network parameters due to fewer variables for training [49]. All ANFIS have similar settings and the synchronization of the feed data to all ANFIS networks is very important and should be considered in practice. The conventional method for setting parameters in an ANFIS is the gradient descent method. Gradient descent-based methods suffer the defects such as being trapped in a local minimum and failure of the method in non-differentiable functions. To overcome these disadvantages and obtain optimal values of ANFIS parameters, the proposed scheme in this paper uses the grasshopper optimization algorithm instead of using Gradient descent method. The optimization algorithm parameters are specified in Table 1.

Table (1): Optimization algorithm parameters

Architecture	ANFIS
Learning Algorithm	GOA
Population size	5-30
Number of membership function	5-15
Upper and lower boundaries	[-1 1]
Generation	30-150

In this paper, 30 different operating scenarios are considered for state estimation, which generation and

consumption of each scenario is different from the others. In all of these 30 different scenarios, the necessary data for state estimation, including

the measurements of the power injection at the buses (active and reactive power injected into the bus) and the lines flow (active and reactive power flow of the lines), as well as state variables (bus voltage phasors) are captured and considered as training data for the ANFIS. The number of measured samples in each scenario is twice the total number of lines and buses. For example, the IEEE test system has 118 buses and 186 lines in the case of a 118-bus system and 14 buses and 21 lines in the case of a 14-bus system, so the number of training samples in each scenario will be equal to 608 for a 118-bus system and 70 for a 14 bus system. The total number of samples in 30 scenarios for the 118 and 14-bus systems is 18240 and 2100 samples respectively.

We split out 90% of the measured data as training data and 10% as test data. In other words, data from 27 scenarios are considered training data, and data of 3 scenarios will be for test data. The work process is such that the measured data related to the state variables at each bus, are separated and applied to the ANFIS associated with that bus. Each ANFIS estimates the state variables of the corresponding bus.

In the following, the added capability to the proposed plan allows providing the appropriate state estimation

when incomplete data are transmitted to the control center due to the disconnection or failure of measurement devices. As the duration of the state estimation process is limited and short, the missing data recovery should be performed in the shortest possible time. For this purpose, the GMDH neural network is used to recover the missed data. Maintaining the accuracy of approximation and estimation, in addition to high speed, is the most important feature of the GMDH neural network. The principal procedure of the GMDH neural network, like GA, is based on the idea of natural selection, that in each iteration, a number of good and better populations are selected [50, 51]. The recovery process of missed data is described as follows. The measurements needed for the state estimation include active and reactive power injections into the bus and active and reactive power flows through the lines. In the case of missed data, it is assumed that the measurement data of one or more buses are not available. The active power flow in the lines related to each bus can be approximated properly by measuring at the other end of the line.

However, the difference in reactive power at the beginning and end of the lines may be significant because of various operating conditions and different devices such as compensating capacitors in the power system. To recover the reactive power of the lines in which the defect in reactive power measurement exists, the reactive powers measured in other lines are given as GMDH neural network input and its output is the reactive power of the line or lines with the defect data. As mentioned above, 30 different operating scenarios are defined for the state variable estimations of IEEE 14-bus and 118-bus. Active and reactive power injections at the bus, and active and reactive power flow of the lines in these 30 scenarios, are measured and used to train the GMDH neural network. The trained GMDH neural network can be used for missing data recovery in case of device disconnection or failure. Another GMDH neural network is trained similarly and used to recovery the missed data related to injected active and reactive power of the buses.

Figures 3-a and 3-b completely illustrate the implementation process of the proposed plan.

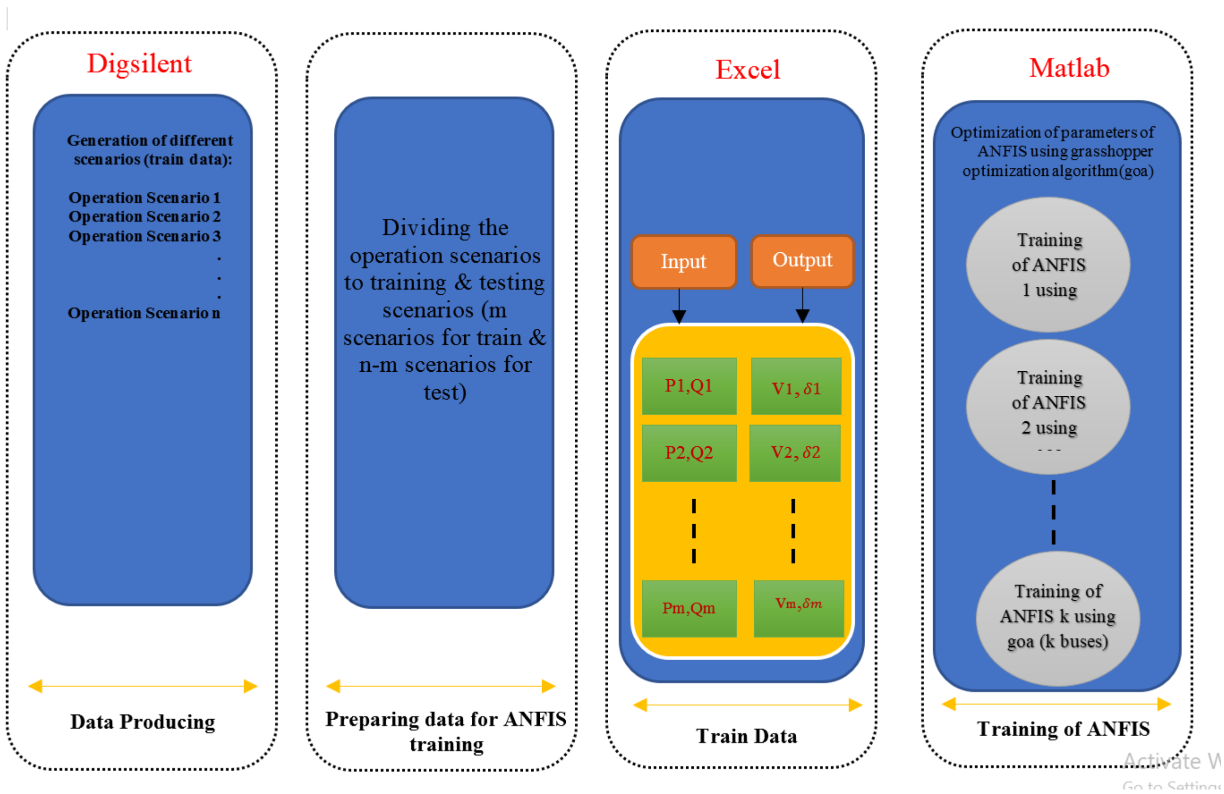

Figure. 3-a. How to train ANFIS

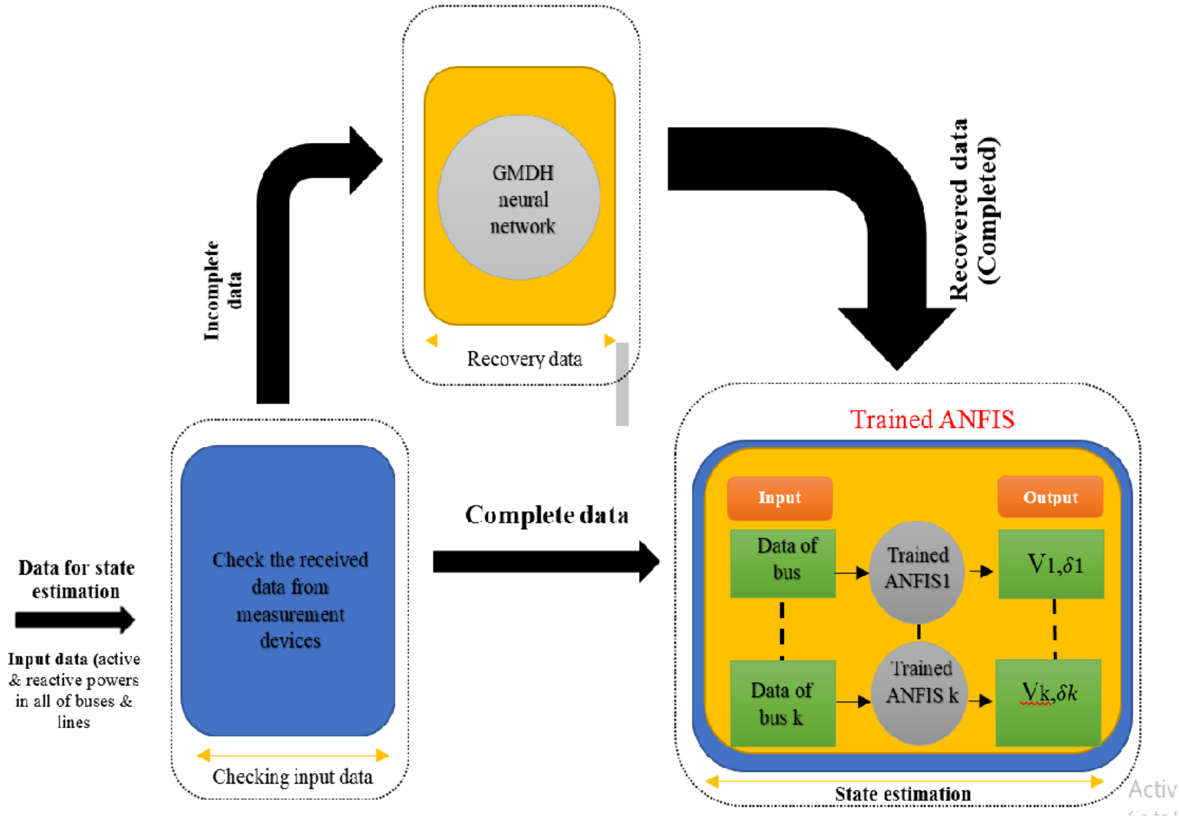

Figure. 3-b. Performance of the proposed state estimation plan when facing new data

4.1. Gaussian White Noise (WGN)

In practice, the measured values for state estimation have errors. In simulations, these measured values are error-free, and to bring simulation closer to real-world conditions, we need to add some values to simulations as errors. White Gaussian noise is a criterion that is added to measured values of power injection at the bus and power flow in the lines as an error with zero mean and standard deviation equals one. The standard deviation of Gaussian noise for active and reactive power injection is 0.05 and for active reactive power flow is 0.001. The Gaussian white noise is formulated as follows:

$$Z_s(t) = Z(t) + rand \times k \times \sigma + \mu \qquad (18)$$

Z_s (t) and $Z(t)$ respectively indicate the measurements after and before adding Gaussian white noise at the instant t. Coefficient k determines the measurement error. k = 0, there is no error in the measurement. σ is the standard deviation and μ is the mean that is considered zero [15]. The standard deviation will be increased by zero mean and the following standard deviation, $\sigma_{\mathbf{injections}}$ = k×0.05 and $\sigma_{\mathbf{flows}}$ = k×0.001. This paper considers k = 1 ... 5.

5. Results and Discussion

One of the important features of the proposed plan is its ability to provide appropriate state estimation in both complete and incomplete (missed) data conditions. So, the results are divided into two subsections, results in complete data condition and results in incomplete data condition.

5.1. State estimation in complete data condition

In this section, the results related to the complete data condition are presented. Table 2 shows the results of the state estimation (magnitude and angle of the voltage) for the IEEE 14-bus system. Given these results, with k=1, the MSE and MAPE of the proposed plan for estimating the voltage magnitude are 2e-4 and 0.7 respectively, and for estimating the voltage angle are 3.77e-3 and 3.0.07, respectively. With k = 2, MSE and MAPE for voltage magnitude are obtained 4e-2.86 and 0.84, respectively, and for angle are 3e-3.98 and 3.15, respectively. With k = 1-5, the obtained MSE and MAPE are presented in Table 2. According to Table 2, with the increase of the k value, which is equivalent to increasing the error rate of the measuring devices, the growth of the estimation error is also observed. The MSE and MAPE obtained for different values of k are basically the means of MSE and MAPE of the voltage magnitude and angle at all buses. Figures 4 and 5 show the results of the state estimation (voltage magnitude and angle) in a diagram proportional to the increase in the error of the measuring devices.

The convergence time of the ANFIS in the training process is presented in Table 3. Given this table, convergence and state estimation times basically are the mean of convergence and estimation times of parallel ANFIS for the IEEE 14-bus system. From the time of the ANFIS convergence in the training process and as well as the time of state estimation, it is clear that the proposed plan can be used as an online stated estimator; because the state estimation is performed in a very short time.

The results of the state estimation for the modified IEEE 118 bus system are presented in Table 4. Figures 6 and 7 show the results of the state estimation (the magnitude and angle of the bus voltages) in a diagram proportional to the growth of the measuring device error. The convergence and training times of ANFISes are represented in Table 5. It should be noted that the table's bottom row shows the number of function evaluations. This row indicates that the used algorithms for optimizing and training the ANFIS have been implemented several times during the training process. The number of the measured variables in the modified IEEE 118-bus system is greater than in the IEEE 14-bus system. However, the proposed plan keeps its efficiency in larger systems with more data, both in terms of the speed and accuracy of the estimation.

The specifications of the computer system used are Intel(R) Core(TM) i7-6500U CPU @2.50GHz 2.60GHz, RAM 8.00 GB.

Table (2): Stats estimation results for the IEEE 14-bus system in complete data condition

IEEE 14 bus	$\varepsilon\delta$			εV		
K	MSE (p.u)	MAPE (%)	std	MSE (p.u)	MAPE (%)	std
1	3.77e-3	3.07	0.061	2e-4	0.7	0.014
2	3.98e-3	3.15	0.063	2.86e-4	0.84	0.0169
3	4.23e-3	3.25	0.065	3.33e-4	0.91	0.0182
4	4.67e-3	3.41	0.069	4e-4	1	0.02
5	5.01e-3	3.53	0.071	4.73e-4	1.08	0.0217

Table (3): Convergence and estimate times of ANFIS

IEEE 14 bus	ANFIS _GOA	
	$\varepsilon\delta$	εV
Mean time to convergence (s)	4.3	4.3
Mean time to estimation (s)	0.281	0.29
Number of function evaluations	2635	2635

Table (4): State estimation results for the IEEE 118-bus system in complete data condition

IEEE 118 bus modified	$\varepsilon\delta$			εV		
K	MSE (p.u)	MAPE (%)	std	MSE (p.u)	MAPE (%)	std
1	5.84e-3	3.82	0.076	8.51e-8	0.0145	2.91e-4
2	6.13e-3	3.91	0.078	9.81e-8	0.0156	3.13e-4
3	6.94e-3	4.16	0.083	2.01e-7	0.0224	4.48e-4
4	7.61e-3	4.36	0.087	4.43e-7	0.0332	6.65e-4
5	8.83e-3	4.69	0.094	5.9e-7	0.0385	7.7e-4

Table (5): Convergence and estimate times of AN

IEEE 118 bus modified	ANFIS _GOA	
	$\varepsilon\delta$	εV
Mean time to convergence (s)	5.32	4.054
Mean time to estimation (s)	0.3	0.284
Number of function evaluations	2635	2635

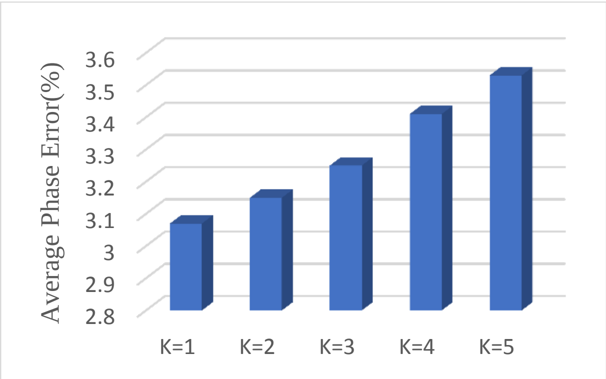

Figure 4. Mean Absolute Percentage Error (MAPE) of angle for the IEEE 14-bus system in complete data condition

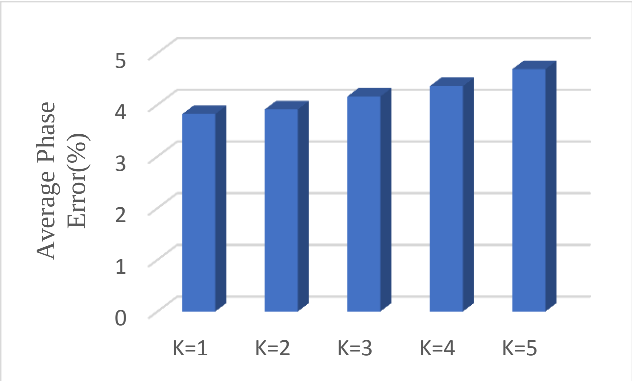

Figure 6. Mean Absolute Percentage Error of angle for the modified IEEE 118-bus system in complete data condition

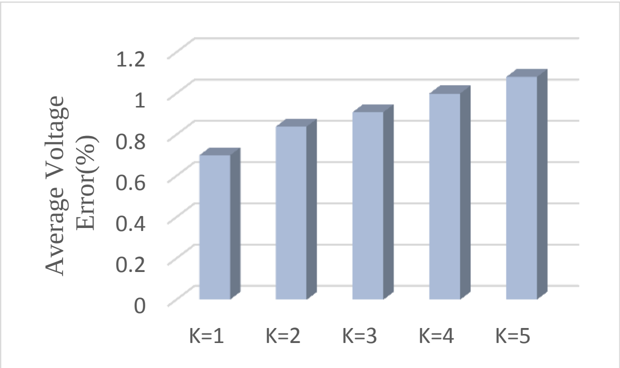

Figure 5. Mean Absolute Percentage Error (MAPE) of voltage for the IEEE 14-bus system in complete data condition

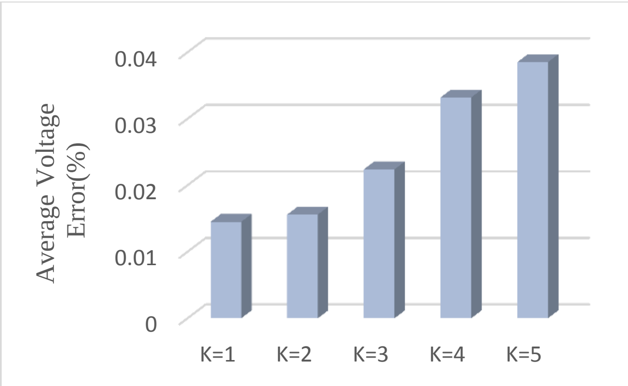

Figure 7. Mean Absolute Percentage Error of voltage for the modified IEEE 118-bus system in complete data condition

5.2. State estimation in incomplete data condition

In this section, we assume that the measurement data of the given bus including the power injection at buses and power flow through the lines are not available. The active power flow in the lines can be approximated by measuring them at the other end of the line, but the values of power injection and reactive power flow of the lines must be retrieved. It is assumed that these missed measurements occurred at one of the buses in each of the two systems, and the data at a bus should be determined. Based on the assumption, power injections respectively at bus 4 in IEEE 14-bus system and at bus 17 in IEEE 118-bus system are unknown. By using the GMDH neural network, power injections at buses with missed data are recovered with those related to buses under normal conditions. Tables 6 and 7 show the results of missed data recovery in 5 different operating conditions of test systems. These different operating conditions point to the power generation and consumption of each operating condition being different from others. In other words, the power system is assumed to be dynamic. In each of the five operating conditions, the power injections at buses with the missed data have been recovered and are given as inputs of the proposed plan for state estimation. Figures 8 and 9 show the mean absolute percentage error of recovery data related to power injections at given buses. The results of the state estimations of the buses with missed data are shown in Tables 8 and 9 and Figures 10 and 11.

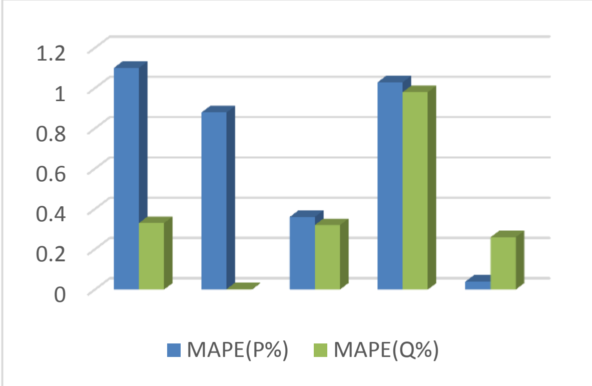

Figure. 8. Mean absolute percentage error of missed data recovery related to power injections at bus 4 of IEEE 14-bus system

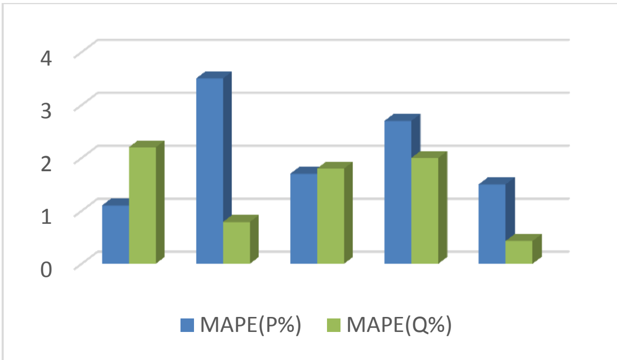

Figure .9. Mean absolute percentage error of missed data recovery related to power injections at bus 17 of the modified IEEE 118-bus system

Table (6): Missed data recovery including active power and reactive power at bus 4 of IEEE 14-bus system

IEEE 14 bus (4)	Active Power			Reactive Power		
Number of different operation modes	P_{true} (MW)	P_{est}(MW)	MAPE(%)	P_{true} (MW)	P_{est}(MW)	MAPE(%)
1	110.02	108.91	1.1	-17.32	-17.3257	0.33
2	134.36	133.17	0.88	-17.83	-17.829	0.003
3	121.33	120.9	0.36	-19.53	-19.5362	0.32
4	121.33	120.09	1.029	-17.83	-18	0.98
5	110.01	109.97	0.04	-22.55	-22.6	0.26

Table (7): Missed data recovery including active power and reactive power at bus 17 of the modified IEEE 118-bus system

IEEE 118 bus (17)	Active Power			Reactive Power		
Number of different operation modes	P_{true} (MW)	P_{est}(MW)	MAPE(%)	P_{true} (MW)	P_{est}(MW)	MAPE(%)
1	230.66	228.13	1.1	71.42	69.85	2.2
2	220.83	223.11	3.5	73.41	72.84	0.79
3	250	245.75	1.7	66.46	65.27	1.8
4	209	203.36	2.7	67.38	66.04	2
5	240.53	236.96	1.5	62.58	62.32	0.43

Table (8): Results of the state estimation at bus 4 in IEEE 14-bus system in missed data condition

Est bus 4	$\varepsilon\delta$		εV	
Number of different operation modes	MSE(p.u)	MAPE(%)	MSE(p.u)	MAPE(%)
1	1.6e-6	0.063	4.1e-5	0.32
2	1.1e-6	0.052	2.3e-6	0.075
3	1.2e-5	0.17	5.2e-6	0.11
4	1.4e-5	0.187	3.9e-5	0.31
5	3.2e-6	0.089	3.1e-6	0.088

Table (9): Results of the state estimation at bus 17 in IEEE 118-bus system in missed data condition

Est bus 17	$\varepsilon\delta$		εV	
Number of different operation modes	MSE(p.u)	MAPE(%)	MSE(p.u)	MAPE(%)
1	2.7e-7	0.026	9.3e-8	0.015
2	5.86e-6	0.12	1.1e-7	0.016
3	5.86e-6	0.12	1.7e-7	0.02
4	1.5e-4	0.61	4e-7	0.031
5	3.2e-7	0.028	1.1e-7	0.061

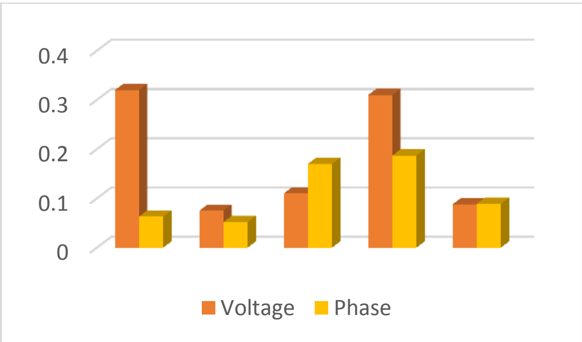

Figure 10. Mean absolute percentage error of the state estimations in missed data condition at bus 4 of IEEE 14-bus system

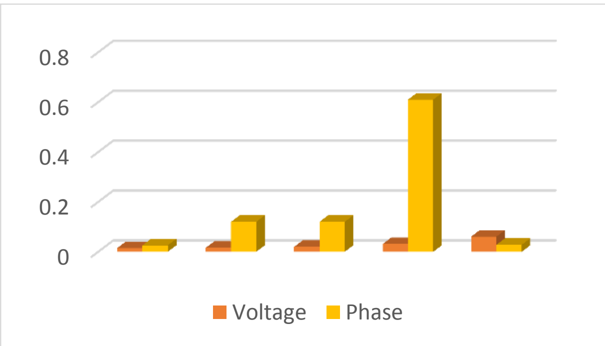

Figure 11. Mean absolute percentage error of state estimations in missed data condition at bus 17of the modified IEEE 118-bus system

6. Comparison of the proposed plan with other methods

In this section, the results of the proposed plan are compared with the results of other methods implemented in [15] and [16]. In [15], the combination of the MLP neural network with the SFS algorithm was used to state the estimation of the networks that are the same as ours. The authors in [16] used a combination of the CCN method and the GA algorithm for state estimation. The test network in [15] is IEEE 68-bus network. Tables 10 and 11 show the comparison between the results of the proposed plan with [15] and [16]. According to Table 10, it is founded that in IEEE 14-bus system, the accuracy of bus angle estimation by the proposed plan is lower than the method of [15], but our plan has a higher accuracy at the voltage magnitude estimation. In IEEE 118-bus system, the proposed plan accuracy, either in the angle or in the magnitude estimation of the voltage, is better than [15]. Evidently, the accuracy range of the voltage phasor estimation in the two test systems is the same; but the time of convergence and the time of state estimation in our proposed plan is less than [15]. By applying the proposed plan to the 118-bus system, we obtained much lower convergence estimation times than [15]. This will enable the proposed method to be used online too. Given Table 11, the test system of [14] is not the same as our paper. According to Table 10, the accuracy of power system state estimation for 14 and 118 bus test systems obtained by our proposed plan approximately are in the same range and the proposed plan estimates the state variables independent of system size. Therefore, the proposed plan can be compared with reference [16]. The high accuracy and low convergence time of the proposed plan compared to [16] show its superiority

7. Conclusion

Various methods are used for the state estimation of the power system. In this paper, we suggested a new plan for this purpose. An individual ANFIS was considered for each bus as the main tool for state estimation to increase the accuracy of the state estimation results. The conventional method for setting the ANFIS parameters is gradient descent; however, we used an optimization algorithm for this purpose to improve the accuracy of training. The proposed plan is capable to provide an appropriate estimate in the case of missed data. GMDH neural network was used for the recovery of missed data. For IEEE 14-bus system, the accuracy and calculation time for voltage magnitudes and angles are 0.906%, 3.28% and 0.29 seconds, 0.281 seconds respectively For IEEE 118-bus system, the accuracy and calculation time for voltage magnitudes and angles are 0.0248%, 4.18%, and 0.284 seconds, 0.3 seconds, respectively. Comparing the proposed plan with the other methods indicated its good conditions. The simulations of the ANFIS and the GMDH neural network were successfully performed with Matlab 2019b software.

Table (10): Comparison of the proposed plan with MLP_SFS in normal condition

	Proposed Plan		MLP_SFS	
IEEE 14 bus	$\boldsymbol{\delta}$	V	$\boldsymbol{\delta}$	V
MAPE (%)	3.28	0.906	1.428	0.98
Mean time to convergence(s)	4.3	4.3	8.88	8.88
Mean time to estimation(s)	0.281	0.29	1.544	1.544
Number of Population	[5-30]	[5-30]	[10-200]	[10-200]
IEEE 118 bus	$\boldsymbol{\delta}$	V	$\boldsymbol{\delta}$	V
MAPE (%)	4.18	0.0248	4.93	3.23
Mean time to convergence(s)	5.32	4.054	31.298	31.298
Mean time to estimation(s)	0.3	0.284	9.67	9.67
Number of Population	[5-30]	[5-30]	[10-200]	[10-200]

Table (11): Comparison of the proposed plan with CCN-GA in normal condition

	Proposed Plan		CCN_GA		
IEEE 14 bus	$\boldsymbol{\delta}$	V	$\boldsymbol{\delta}$	V	IEEE 68 bus (Case 1)
MSE(p.u)	4.33e-3	3.38e-4	0.0143	0.0143	
Mean time to convergence(s)	4.3	4.3	6.65	6.65	
Mean time to estimation(s)	0.281	0.29			
Number of function evaluations	2635	2635	11238	11238	
IEEE 118 bus	$\boldsymbol{\delta}$	V	$\boldsymbol{\delta}$	V	IEEE 68 bus (Case 2)
MSE(p.u)	7.7e-3	2.83e-7	0.0246	0.0246	
Mean time to convergence(s)	5.32	4.054	18.84	18.84	
Mean time to estimation(s)	0.3	0.284			
Number of function evaluations	2635	2635	28701	28701	

References

[1] G. Wang, G. B. Giannakis, j. Chen, J. Sun. "Distribution system state estimation: An overview of recent developments," *Frontiers of Information Technology & Electronic Engineering*, Vol. 20, No. 1, pp. 4-17, 2019

[2] B. Gou, R. G. Kavasseri. "Unified PMU placement for observability and bad data detection in state estimation," *IEEE Transactions on Power Systems,* Vol. 29, No. 6, pp. 2573-2580, 2014

[3] X. Chen, J. Lin, C. Wan, Y. Song, S. You, Y. Zong, W. Guo, and Y. Li, "Optimal meter placement for distribution network state estimation: A circuit representation based MILP approach," *IEEE Transactions on Power Systems,* Vol. 31, No. 6, pp. 4357-4370, 2016.

[4] O. Ivanov, and M. Gavrilaş, "State estimation with Neural Networks and PMU voltage measurements," *Electrical and Power Engineering (EPE), International Conference and Exposition on. IEEE*, pp. 983-988, 2014.

[5] G. R. Tankasala, S. Sanisetty, and V. K. Vala, "Optimal placement of phasor measurement units for state estimation using artificial intelligence techniques," *International Journal Science Engineering Research*, Vol. 3, No. 2, pp. 1-5, 2012.

[6] Andic, Cenk, Ali Ozturk, and Belgin Turkay. "Power system state estimation using a robust crow search algorithm based on PMUs with limited number of channels," *Electric Power Systems Research,* 217 (2023): 109126.

[7] R. Babu, and B. Bhattacharyya, "An Approach for Optimal Placement of Phasor Measurement Unit for Power Network Observability Considering Various Contingencies," *Iranian Journal of Science and Technology, Transactions of Electrical Engineering*, Vol. 42, No. 2, pp. 161-183, 2018.

[8] S. E. Razavi, H. Falaghi, A. E. Nezhad, M. J. H. Moghaddam, & F. H. Gandoman, "An effective approach for the probabilistic and deterministic multistage PMU placement using cuckoo search: Iran's National Power System," *Iranian Journal of Science and Technology, Transactions of Electrical Engineering,* Vol. *44*, No. 1, pp. 237-252, 2020.

[9] X. Chen, J. Lin, C. Wan, Y. Song, S. You, Y. Zong, W. Guo, and Y. Li, "Optimal meter placement for distribution network state estimation: A circuit representation-based MILP approach," *IEEE Transactions on Power Systems,* Vol. 31, No. 6, pp. 4357-4370, 2016.

[10] M. Ajoudani, A. Sheikholeslami, A. Zakariazadeh, "Modified Weighted Least Squares Method to Improve Active Distribution System State Estimation," *Iranian Journal of Electrical and Electronic Engineering,* Vol. 16, No. 4, pp. 559-572, 2020.

[11] C. Gu, and P. Jirutitijaroen, "Dynamic state estimation under communication failure using kriging-based bus load forecasting," *IEEE Transactions on Power Systems*, Vol. 30, No. 6, pp. 2831-2840, 2015.

[12] E. Manitsas, R. Singh, B. C. Pal, and G. Strbac, "Distribution system state estimation using an artificial neural network approach for pseudo measurement modeling," *IEEE Transactions on Power Systems*, Vol. 27, No. 4, pp. 1888-1896, 2012.

[13] M. B. Do Coutto Filho, and J. C. S. de Souza, "Forecasting-aided state estimation—Part I: Panorama," *IEEE Transactions on Power Systems,* Vol. 24, No. 4, pp. 1667-1677, 2009.

[14] A. Hassannejad Marzouni, and A. Zakariazadeh, "Error Modeling in Distribution Network State Estimation Using RBF-Based Artificial Neural Network," *Iranian Journal of Electrical and Electronic Engineering,* Vol. 16, No. 3, pp. 292-301, 2020.

[15] H. Mosbah, and M. E. El-Hawary, "Optimization of neural network parameters by Stochastic Fractal Search for dynamic state estimation under communication failure," *Electric Power Systems Research* Vol. 147, pp. 288-301, 2017.

[16] M. A. Rahman, and G. K. Venayagamoorthy, "A hybrid method for power system state estimation using Cellular Computational Network," *Engineering Applications of Artificial Intelligence, Vol.* 64, pp. 140-151, 2017.

[17] V. Basetti, A. K. Chandel, and R. Chandel, "Power system dynamic state estimation using prediction based evolutionary technique," *Energy,* Vol. 107, pp. 29-47, 2016.

[18] K. Zor, O. Timur, and A. Teke, "A state-of-the-art review of artificial intelligence techniques for short-term electric load forecasting," *In 2017 6th International Youth Conference on Energy (IYCE)*, pp. 1-7, 2017.

[19] S. Nanchian, A. Majumdar, and B. C. Pal, "Three-phase state estimation using hybrid particle swarm optimization," *IEEE Transactions on Smart Grid*, Vol. 8, No. 3, pp. 1035-1045, 2015.

[20] D. H. Tungadio, J. A. Jordaan, and M. W. Siti, "Power system state estimation solution using modified models of PSO algorithm: Comparative study," *Measurement,* Vol. 92, pp. 508-523, 2016.

[21] F. García-Lagos, G. Joya, F. J. Marín, and F. Sandoval, "Hopfield neural networks for state estimation: parameters, efficient implementation and results," *e & i Elektrotechnik und Informationstechnik,* Vol. 117, No. 1, pp. 4-7, 2000.

[22] J. P. Pandey, and D. Singh. "Application of radial basis neural network for state estimation of power system networks.," *International Journal of Engineering, Science and Technology, Vol.* 2, No. 3, pp. 19-28, 2010.

[23] S. Mohagheghi, G. K. Venayagamoorthy, and R. G. Harley, "Optimal wide-area controller and state predictor for a power system," *IEEE Transactions on Power Systems*, Vol. 22, No. 2, pp. 693-705, 2007.

[24] O. Ivanov, and M. Garvrilaş, "State estimation for power systems with multilayer perceptron neural networks," *Neural Network Applications in Electrical Engineering (NEUREL), 2012 11th Symposium on. IEEE*, pp. 243-246, 2012.

[25] H. Mosbah, and M. El-Hawary, "Multilayer artificial neural networks for real-time power system state estimation," *Electrical Power and Energy Conference (EPEC),* pp. 344-351, 2015.

[26] J. Krstulovic, V. Miranda, A. J. S. Costa, and J. Pereira," Towards an auto-associative topology state estimator," *IEEE Transactions on Power Systems*, Vol. 28, No. 3, pp. 3311-3318, 2013.

[27] P. P. Barbeiro, J. Krstulovic, H. Teixeira, J. Pereira, F. J. Soares, and J. P. Iria, "State estimation in distribution smart grids using autoencoders," *Power Engineering and Optimization Conference (PEOCO), 2014 IEEE 8th International. IEEE,* pp. 358-363, 2014.

[28] P. P. Barbeiro, H. Teixeira, J. Krstulovic, J. Pereira, and F. J. Soares, "Exploiting autoencoders for three-phase state estimation in unbalanced distributions grids," *Electric Power Systems Research, Vol.* 123, pp. 108-118, 2015.

[29] C. Moreira, J. Opara, H. Keko, J. C. Pereira, and V. Miranda, "Reconstructing missing data in state estimation with autoencoders," *IEEE Transactions on Power Systems,* Vol.27, No. 2, pp. 604-611, 2012.

[30] H. Saadabadi, and M. Dehghani, "Large-scale power systems state estimation using PMU and SCADA data," *Electrical Engineering (ICEE), 2016 24th Iranian Conference on. IEEE*, pp. 906-911, 2016

[31] A. Onwuachumba, and M. Musavi, "Eigenvalue-based optimal placement of PMUs in large power systems," *North*

American Power Symposium (NAPS), 2015. IEEE, pp. 1-6, 2015.

[32] D. D. Silalahi, C. E. Reaño, F. P. Lansigan, R. G. Panopio, and N. C. Bantayan, "Using genetic algorithm neural network on near-infrared spectral data for ripeness grading of oil palm (Elaeis guineensis Jacq.) fresh fruit," *Information Processing in Agriculture*, Vol. 3, No. 4, pp. 252-261, 2016.

[33] L. Hu, L. Qin, K. Mao, W. Chen, and X. Fu, "Optimization of neural network by genetic algorithm for flowrate determination in multipath ultrasonic gas flowmeter," *IEEE Sensors Journal*, Vol. 16, No. 5, pp. 1158-1167, 2016.

[34] W. Sun, and Y. Xu, "Using a back propagation neural network based on improved particle swarm optimization to study the influential factors of carbon dioxide emissions in Hebei Province, China," *Journal of Cleaner Production*, Vol. 112, pp. 1282-1291, 2016.

[35] J. R. Zhang, J. Zhang, T. M. Lok, and M. R. Lyu, "A hybrid particle swarm optimization–back-propagation algorithm for feedforward neural network training," *Applied Mathematics and Computation* Vol. 185, No. 2, pp. 1026-1037 2007.

[36] Raeisi Gahrooei, Yaser, and Rahmatallah Hooshmand. "Short-term electricity price forecasting by hybrid mutual information ANFIS-PSO approach," *Computational Intelligence in Electrical Engineering*, 10.1: 63-72, 2019.

[37] M. Aien, M. Rashidinejad, S. Kouhi, M. Fotuhi-Firuzabad, and S. N. Ravadanegh, "Real-time probabilistic power system state estimation," *International Journal of Electrical Power & Energy Systems*, Vol. 62, pp. 383-390, 2014.

[38] H. Karimipour, V. Dinavahi, "Extended Kalman filter-based parallel dynamic state estimation," *IEEE Transactions on Smart Grid*, Vol. 6, No. 3, pp. 1539–1549, 2015.

[39] J. Zhang, G. Welch, G. Bishop, Z. Huang, "A two-stage Kalman filter approach for robust and real-time power system state estimation," *IEEE Transactions on Sustainable. Energy*, Vol. 5 No. 2, pp. 629–636, 2014.

[40] K. R. Shih, and S. J. Huang, "Application of a robust algorithm for dynamic state estimation of a power system," *IEEE Trans. Power Syst*, Vol. 17, No. 1, pp. 141–147, 2002.

[41] Z. Kazemi, A. A. Safavi. " An Effective Attack-Resilient Kalman Filter-Based Approach for Dynamic State Estimation of Synchronous Machine." *Iranian Journal of Electrical and Electronic Engineering*, Vol. 16, No. 3, pp. 279-291, 2020.

[42] M. Khodsuz, S. Seyyedbarzegar. "Surge Arrester Monitoring under Different Operating Conditions Using Bees-ANFIS," *Iranian Journal of Electrical and Electronic Engineering* Vol. 15, No. 1, pp. 151-160, 2019.

[43] Sarkar, Sobhan, Anima Pramanik, and J. Maiti. "An integrated approach using rough set theory, ANFIS, and Z-number in occupational risk prediction." *Engineering Applications of Artificial Intelligence*, 117, 105515, 2023.

[44] O. B. Adewuyi, K. A. Folly, D. T. O. Oyedokun and E. I. Ogunwole "Power system voltage stability margin estimation using adaptive neuro-fuzzy Inference system enhanced with particle swarm optimization," *Sustainability*, Vol. 14, pp. 1-17, 2022.

[45] M. M. Zabihi Shesh Poli, M. Aliyari Shoorehdeli, and A. Moarefianpour. "Lyapunov stability analysis in the training of type 2 Neuro-Fuzzy Identifier with a swarm-based hybrid intelligent algorithm." *Computational Intelligence in Electrical Engineering* Vol.12, No. 4, pp.73-87, 2021.

[46] A. Ghaghishpour, A. Koochaki and M. Radmehr, "Online voltage stability margin assessment using optimized adaptive ANFIS and wavelet transform based on principal component analysis". *Computational Intelligence in Electrical Engineering*, Vol.13, No. 2, pp. 83-102, 2022.

[47] M. A. Soliman, H. M. Hasanien, H. Z. Azazi, E. E. El-Kholy, and S. A. Mahmoud, "Hybrid ANFIS-GA-based control scheme for performance enhancement of a grid-connected wind generator," *IET Renewable Power Generation*, Vol. 12, No. 7, pp. 832-843, 2018.

[48] S. Saremi, S. Mirjalili, and A. Lewis, "Grasshopper optimization algorithm: theory and application." *Advances in Engineering Software*, Vol. 105, pp. 30-47, 2017.

[49] H. Salehfar, and R. Zhao, "A neural network pre estimation filter for bad-data detection and identification in power system state estimation," *Electric Power Systems Research*, Vol. 34, No. 2, pp. 127-134, 1995.

[50] M. Zareb, W. Nouibat, Y. Bestaoui, R. Ayad, and Y. Bouzid, "Evolutionary Autopilot Design Approach for UAV Quadrotor by Using GA," *Iranian Journal of Science and Technology, Transactions of Electrical Engineering*, Vol. 44, No. 1, pp. 347-375, 2019.

[51] Fakharian, Pouyan, et al. "Compressive strength prediction of hollow concrete masonry blocks using artificial intelligence algorithms," *Structures*. Vol. 47. Elsevier, 2023.